

Supplement of Earth Syst. Sci. Data, 15, 5171–5181, 2023
<https://doi.org/10.5194/essd-15-5171-2023-supplement>
© Author(s) 2023. CC BY 4.0 License.



Open Access
Earth System
Science
Data

Supplement of

A global zircon U–Th–Pb geochronological database

Yujing Wu et al.

Correspondence to: Jianqing Ji (grsange@pku.edu.cn)

The copyright of individual parts of the supplement might differ from the article licence.

Outline

1. Methods

2. Figures

Figure S1. Error fitting curves of different ages derived from LA-ICP-MS.

5 Figure S2. Error fitting curves of different ages derived from SHRIMP.

Figure S3. Error fitting curves of different ages derived from SIMS.

Figure S4. Error fitting curves of different ages derived from TIMS.

Figure S5. Probability distribution functions (PDF) of proximity and probability values.

Figure S6. Zircon production series since 4.4 Ga (not weighted based on spatiotemporal density).

10 Figure S7. Zircon production series in the Phanerozoic (not weighted based on spatiotemporal density).

Figure S8. Spatial distribution of detrital zircons.

Figure S9. Spatial distribution of igneous zircons.

Figure S10. Spatial distribution of metamorphic zircons.

15 **3. Tables**

Table S1. Error fitting curves for different age types.

Table S2. Age error fitting of different dating instruments.

Table S3. Intersection of age error curves (unit: Ma)

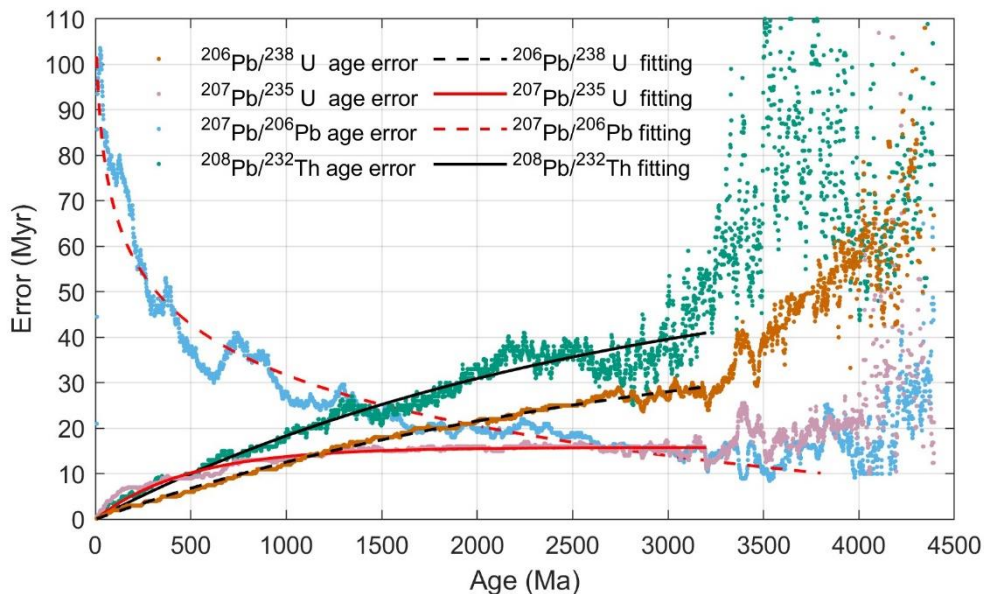
20 **4. References**

1. Methods

25 The zircon U–Th–Pb dating error is related to the zircon age. In this study, the age error within a certain time interval is obtained using the moving average method (Wu et al., 2022). The length of the sliding window (bin size) is the median of all age errors (14 Myr), and the sliding step size is 1 Myr. For each age type, when the window slides along the time axis, the median of the age error in each window is counted and assigned to the middle age of the window. Then, we can obtain an error-age scatter diagram (see Figure 2). When the sample is too old, the dating uncertainty of all age types increases significantly, which may be attributed to sample preservation. Then, the error points for various ages were fitted to obtain error curves (see the equations in Table S1).

30 Zircon production increases with magmatic and metamorphic activities. Therefore, the amount of zircon production can be used to understand the past intensity of geological activity (Arndt and Davaille, 2013). A simple and direct proxy is the number of zircon age records for different geological times, which can indicate the intensity of magmatic and metamorphic activities (Wu et al., 2022). First, we used the noniterative probability model to derive a recommended age for each dating record (Puetz et al., 2021; Puetz and Spencer, 2023). Then, we conducted bootstrap resampling based on the “inverse
35 proximity weighting” to minimize the impact of biased sampling (Mehra et al., 2021; Keller and Schoene, 2012). Based on equations in (Mehra et al., 2021), we calculated the proximity value $w(x)$ which measure the spatiotemporal distance between two data points, and the probability value $P(x)$ which provides a sampling weight for resampling process (Mehra et al., 2021) (Figure S5). The bootstrap resampling procedures are as follows: 1) A subset containing 0.1 million records was randomly selected with probability values $P(x)$ as weights. 2) A simulated dataset for each resampled data was drawn from a
40 Normal distribution according to the recommended age mean and standard deviation. 3) A simulated time series was derived using the moving average method (Wu et al., 2022). 4) Repeat steps 1-3 for 10,000 times, we got the distribution of zircon production series (see Figure 4 and 5).

2. Figures



45 **Figure S1. Error fitting curves of different ages derived from LA-ICP-MS.**

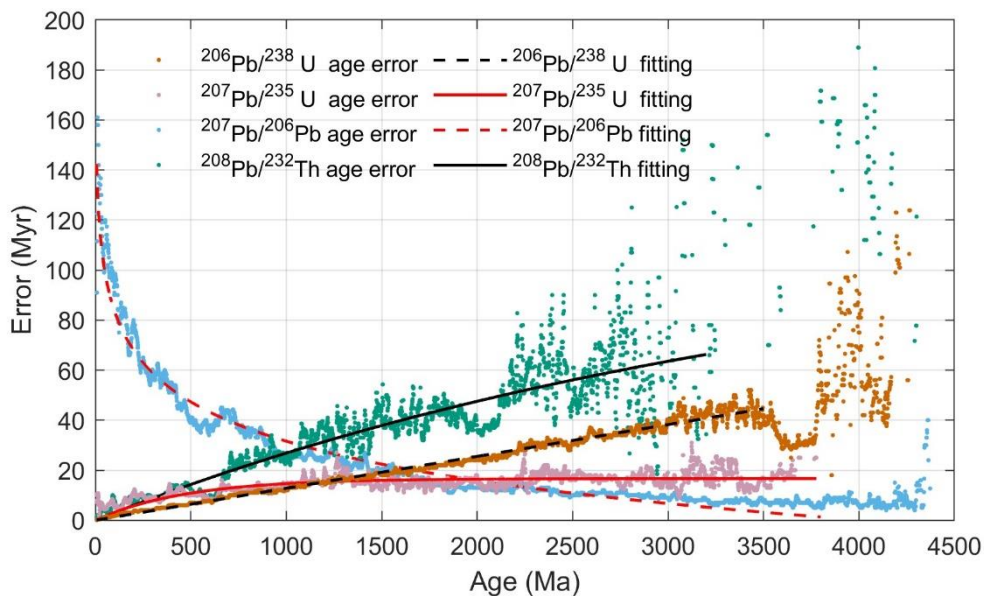


Figure S2. Error fitting curves of different ages derived from SHRIMP.

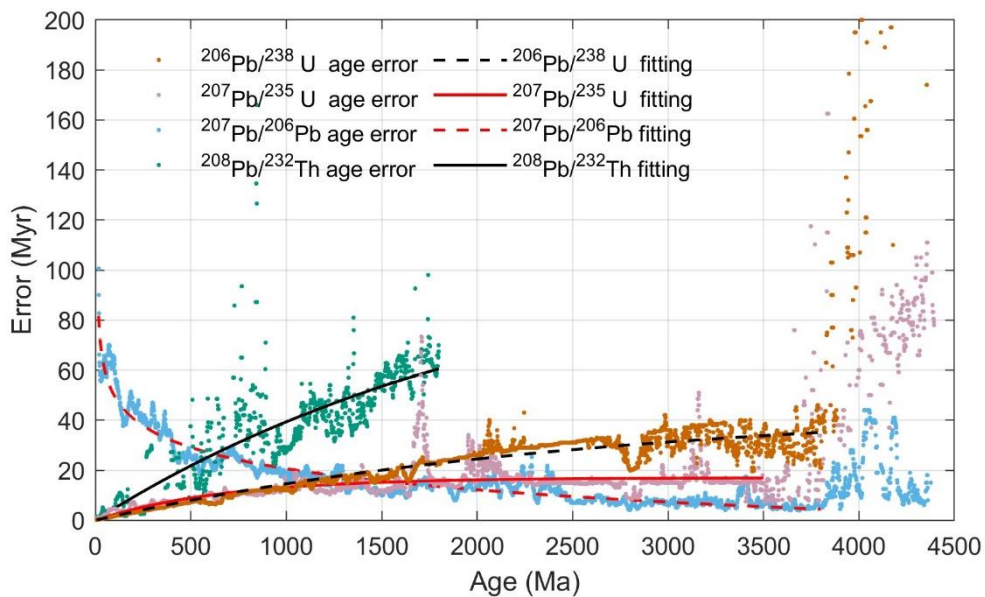


Figure S3. Error fitting curves of different ages derived from SIMS.

50

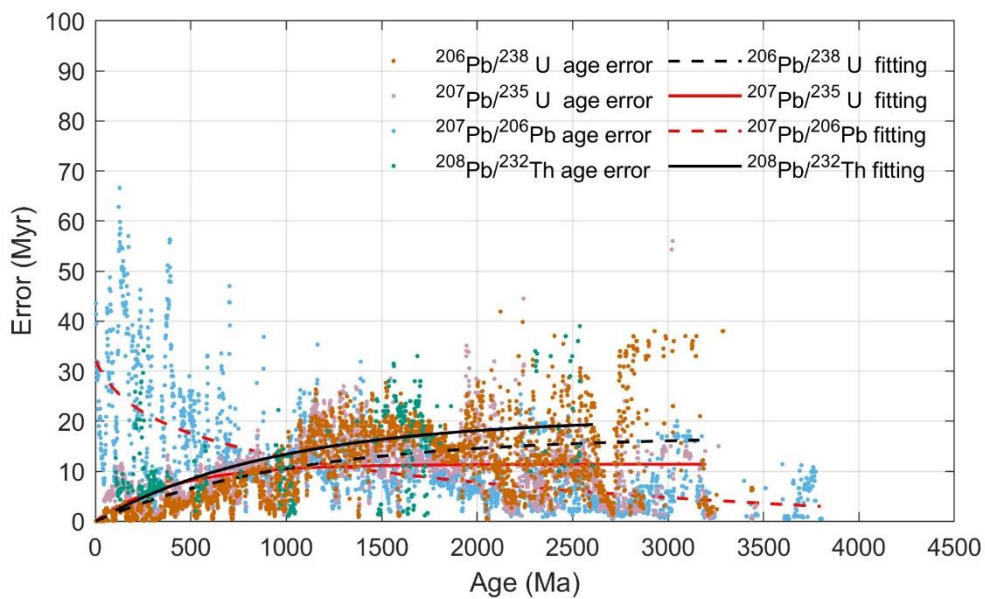
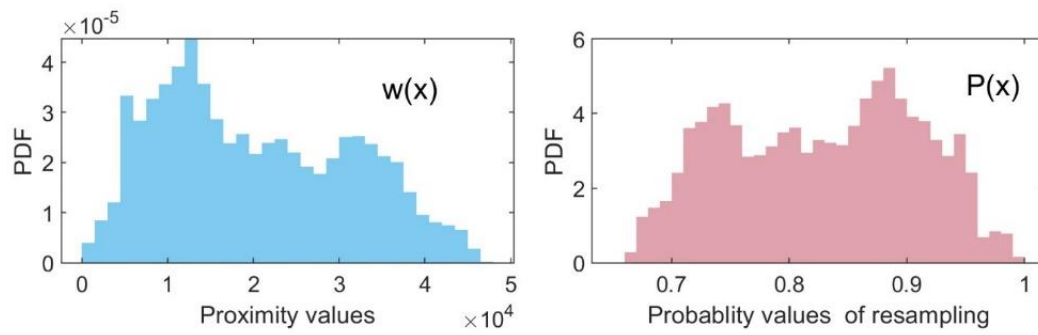
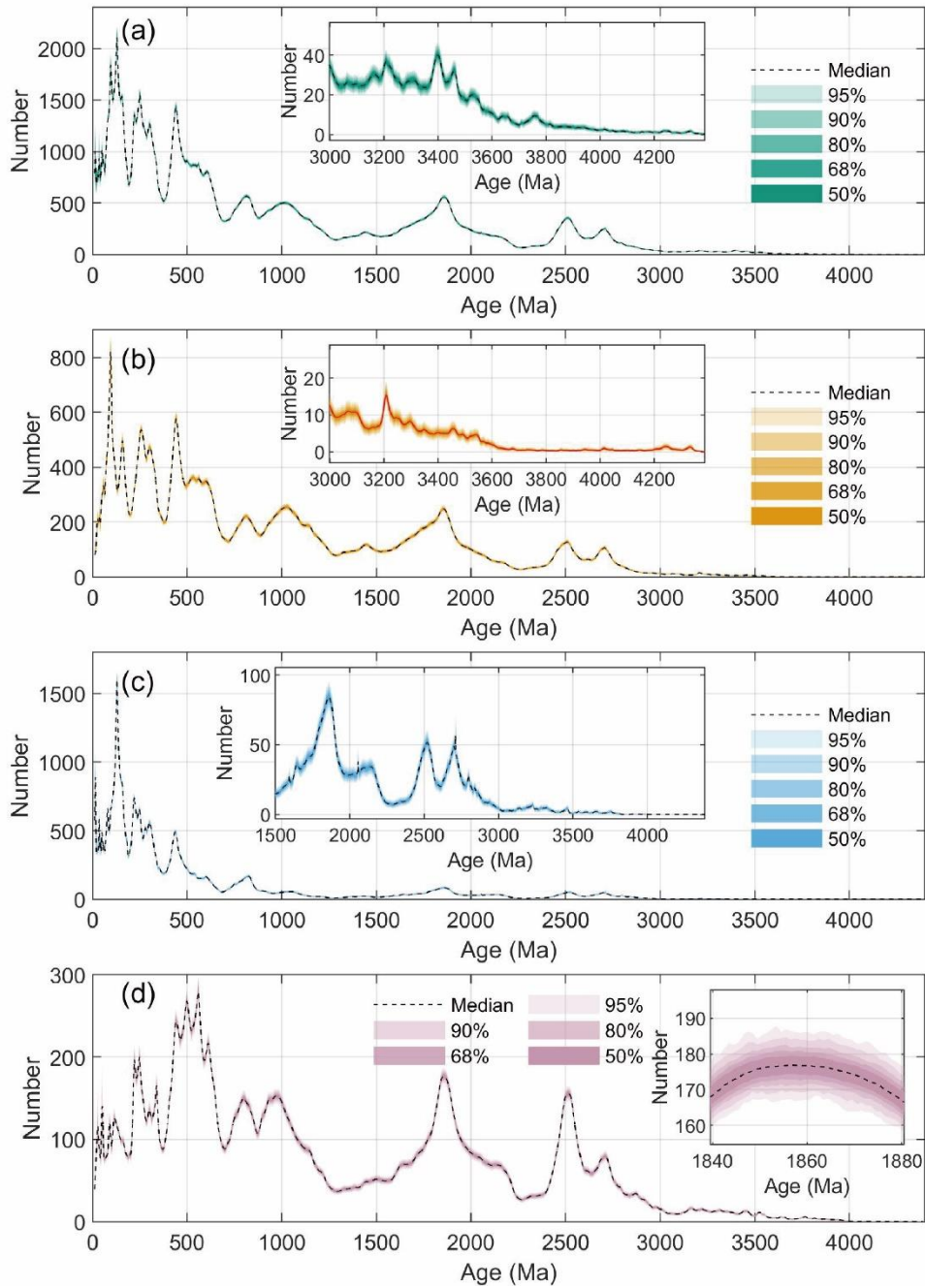


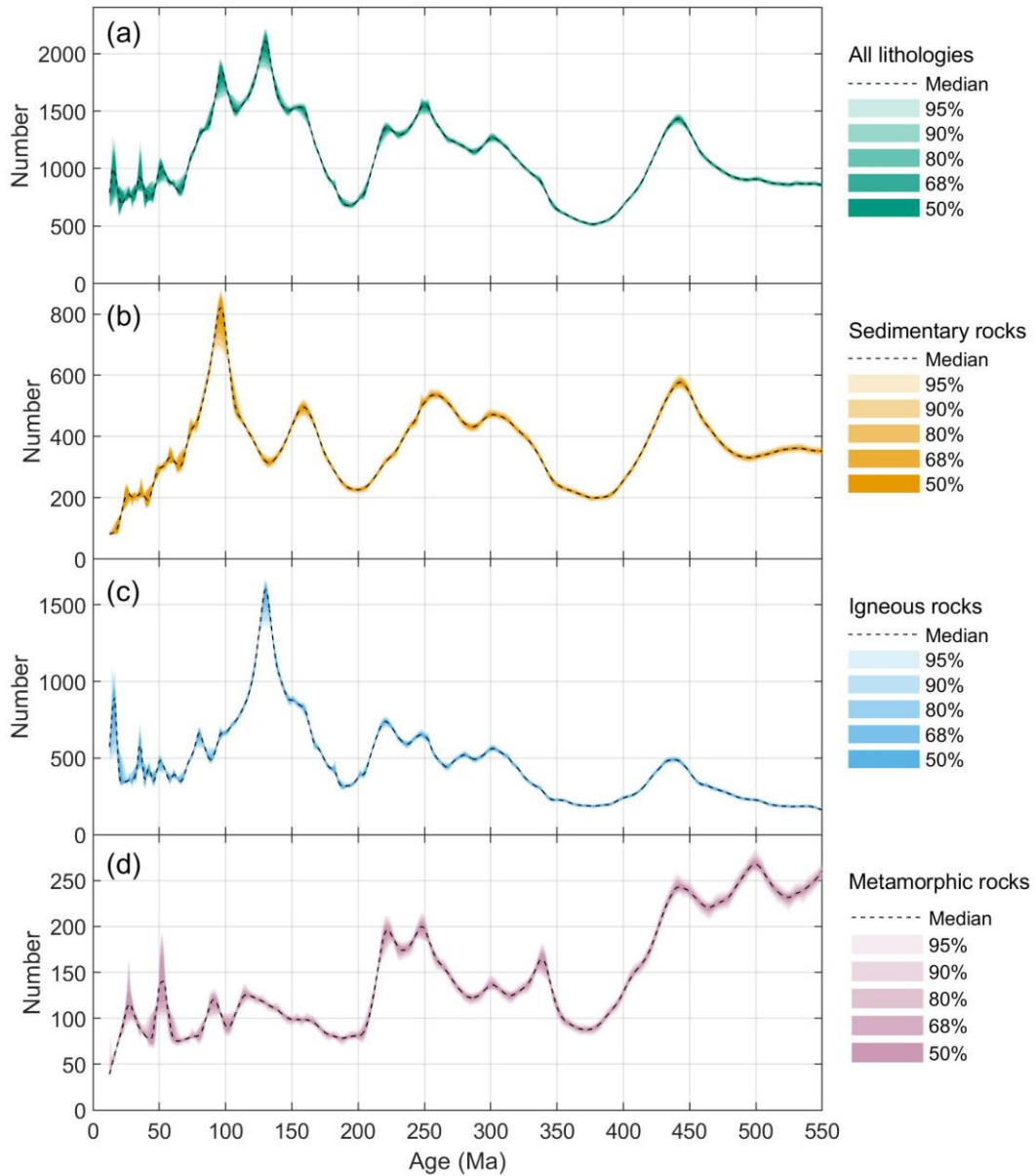
Figure S4. Error fitting curves of different ages derived from TIMS.



55 **Figure S5. Probability distribution functions (PDF) of proximity and probability values. The $w(x)$ and $P(x)$ were calculated using equations in (Mehra et al., 2021). We used a spatial scale of 0.5 degrees and a age scale of 10 Myr.**



60 **Figure S6. Zircon production series since 4.4 Ga (not weighted based on spatiotemporal density). The host rocks of each zircon series are (a) of all lithologies, (b) sedimentary rocks, (c) igneous rocks, and (d) metamorphic rocks. The insets of panels (a-c) focus on the data before 3 Ga. The inset of Panel (d) highlights the impact of dating errors on age series, which can be disregarded, as shown. The filled zones represent 1000 Monte Carlo simulations of the zircon series with different transparencies, indicating different distribution probabilities, as shown in the legend. The dashed line indicates the median of the simulations. In each simulation, simulated zircon ages are selected based on their dating error. For more simulation details, see (Wu et al., 2022).**



65

Figure S7. Zircon production series in the Phanerozoic (not weighted based on spatiotemporal density). The host rocks of each zircon series are (a) of all lithologies, (b) sedimentary rocks, (c) igneous rocks, and (d) metamorphic rocks. The filled zones represent 1000 Monte Carlo simulations of the zircon series with different transparencies, indicating different distribution probabilities, as shown in the legend. The dashed line indicates the median of the simulations. In each simulation, simulated zircon ages are selected based on their dating error. For more simulation details, see (Wu et al., 2022).

70

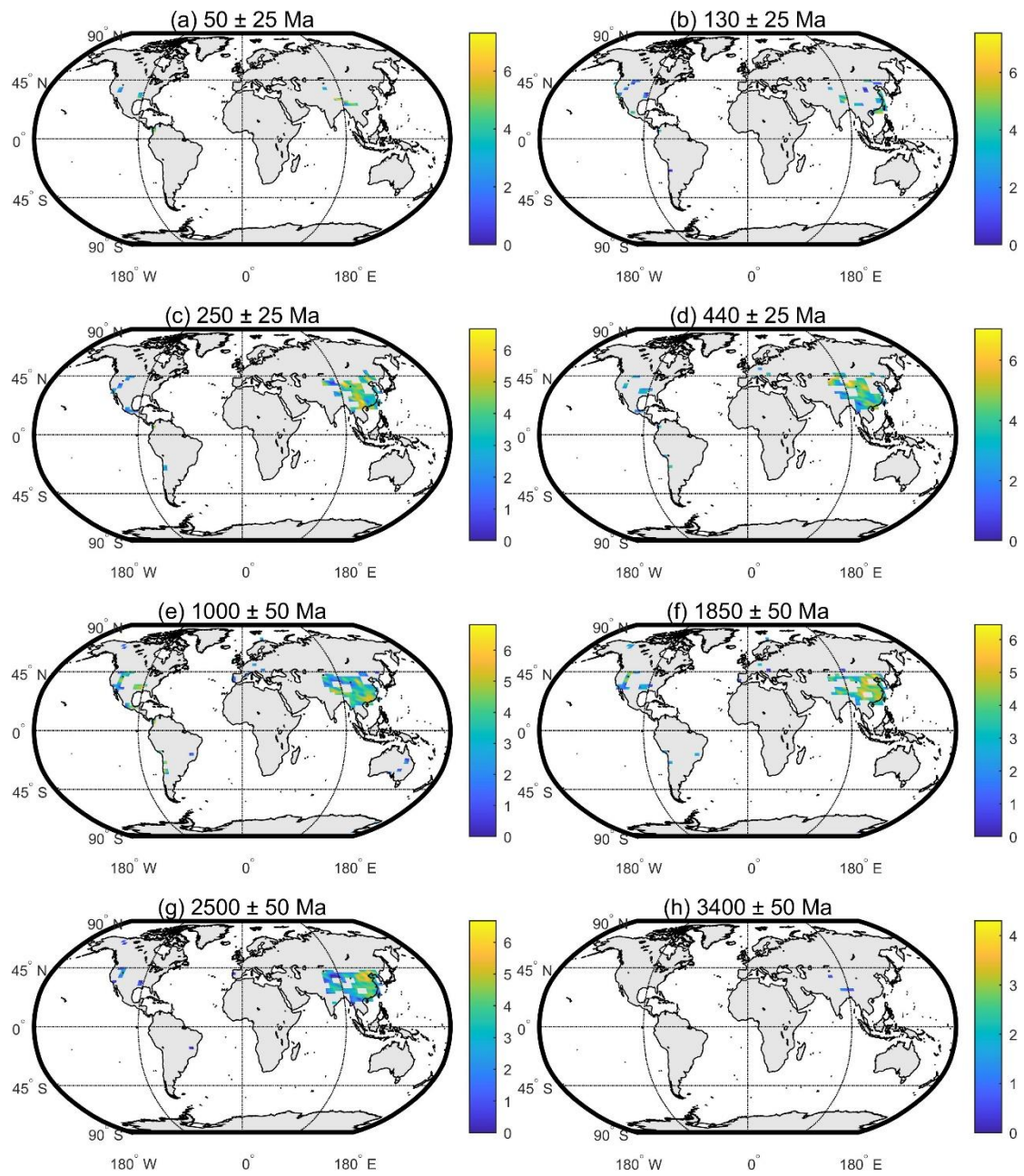
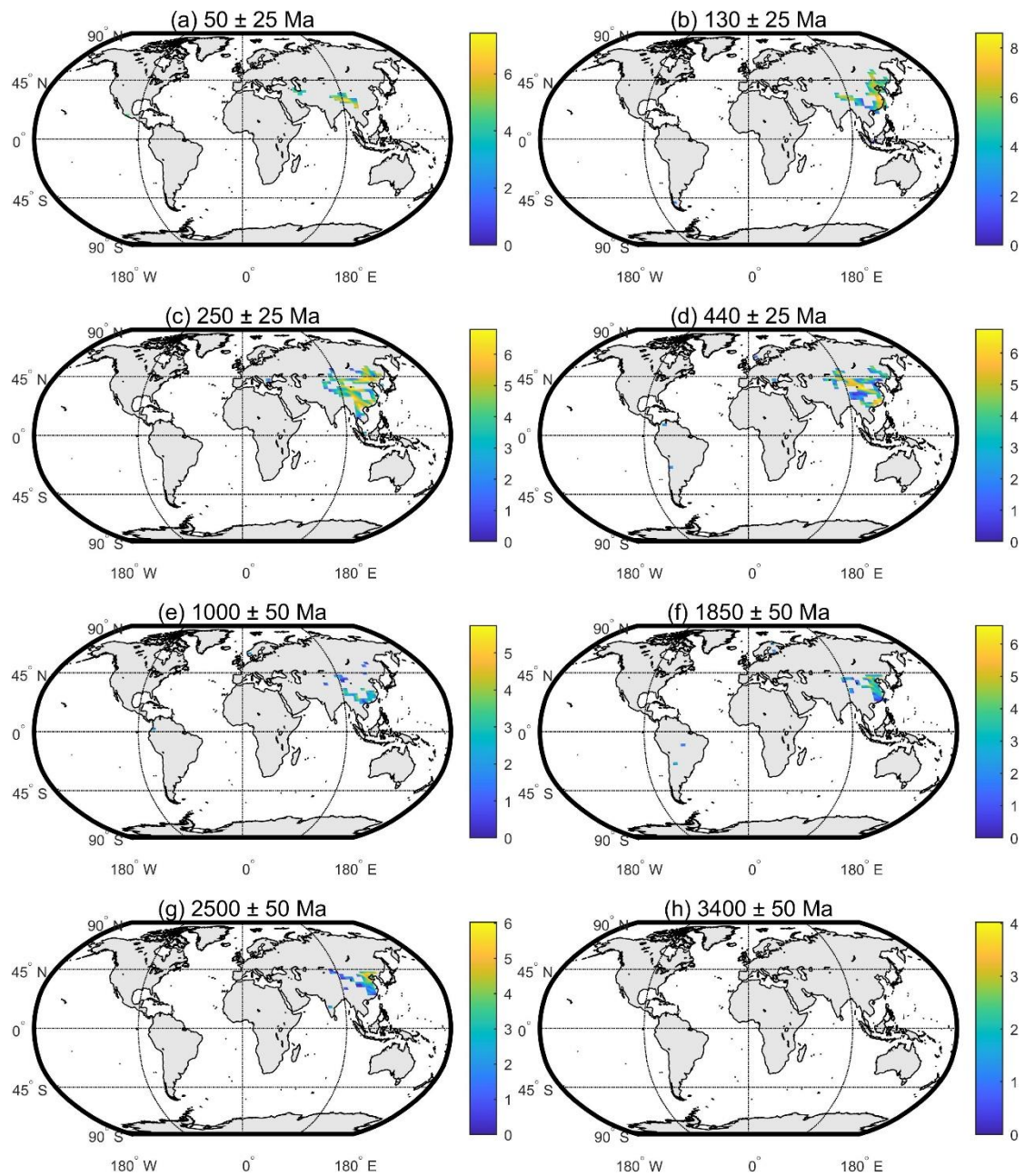


Figure S8. Spatial distribution of detrital zircons. Since some areas were oversampled and old ages are sparse, we should pay more attention to relative rather than absolute zircon densities when comparing regions.



75 **Figure S9. Spatial distribution of igneous zircons. Since some areas were oversampled and old ages are sparse, we should pay more attention to relative rather than absolute zircon densities when comparing regions.**

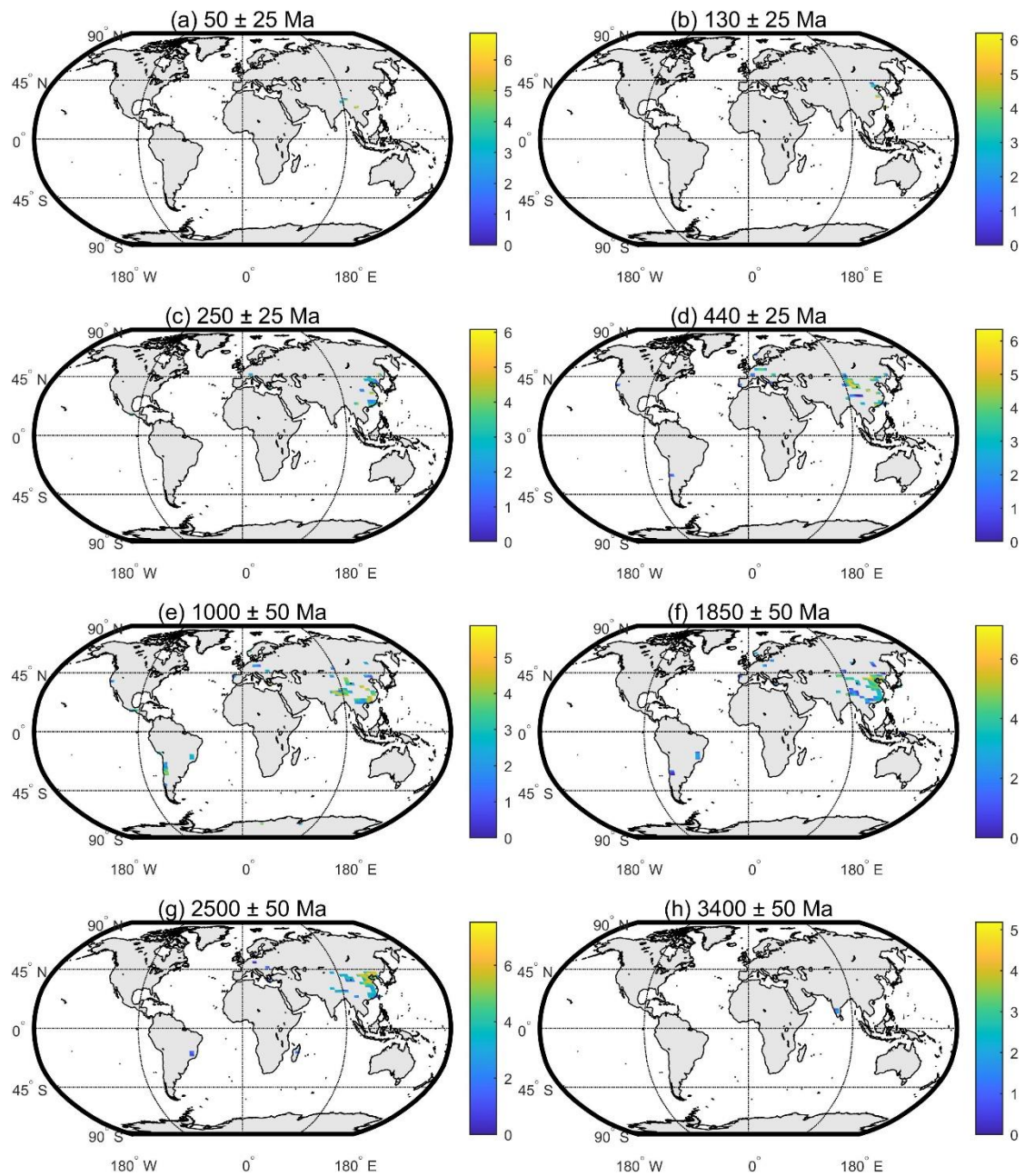


Figure S10. Spatial distribution of metamorphic zircons. Since some areas were oversampled and old ages are sparse, we should pay more attention to relative rather than absolute zircon densities when comparing regions.

Table S1. Error fitting curves for different age types.

Age type	Regression equation	Adjust R-Squared	Parameters with 95% confidence interval (CI)
$^{206}\text{Pb}/^{238}\text{U}$	$y=a*[1-\exp(-b*x)]$	0.9957	a = 56.32 (55.69, 56.95) b = 2.507 (2.470, 2.545) $\times 10^{-4}$
$^{207}\text{Pb}/^{235}\text{U}$	$y=a*[1-\exp(-b*x)]$	0.9417	a = 15.66 (15.62, 15.70) b = 2.066 (2.040, 2.091) $\times 10^{-3}$
$^{207}\text{Pb}/^{206}\text{Pb}$	$y=a-b*\ln(x+c)$	0.9478	a = 148.7 (147.3, 150.1) b = 17.11 (16.92, 17.30) c = 11.90 (8.996, 14.80)
$^{208}\text{Pb}/^{232}\text{Th}$	$y=a*[1-\exp(-b*x)]$	0.9416	a = 59.90 (58.50, 61.29) b = 3.948 (3.803, 4.093) $\times 10^{-4}$

Note: Variable “x” denotes age. Variable “y” denotes age error.

Table S2. Age error fitting of different dating instruments.

Age type	LA-ICP-MS		SHRIMP		SIMS		TIMS	
	Adjust r^2	Parameters with 95% CI	Adjust r^2	Parameters with 95% CI	Adjust r^2	Parameters with 95% CI	Adjust r^2	Parameters with 95% CI
$^{206}\text{Pb}/^{238}\text{U}$	0.9935	a = 44.51 (44.07, 44.94)	0.9842	a = 3568 (-2544, 9680)	0.896	a = 45.76 (44.6, 46.93)	0.3756	a = 17.00 (16.20, 17.80)
		b = 3.318 (3.270, 3.365)		b = 3.591 (-2.590, 9.771)		b = 3.830 (3.666, 3.994)		b = 9.680 (8.537, 1.082)
		$\times 10^{-4}$		$\times 10^{-6}$		$\times 10^{-4}$		$\times 10^{-4}$
$^{207}\text{Pb}/^{235}\text{U}$	0.9370	a = 15.77 (15.72, 15.81)	0.4956	a = 16.65 (16.53, 16.78)	0.3863	a = 17.00 (16.70, 17.30)	0.1674	a = 11.40 (11.11, 11.69)
		b = 2.071 (2.044, 2.097)		b = 2.102 (2.023, 2.181)		b = 1.484 (1.384, 1.585)		b = 2.465 (2.168, 2.762)
		$\times 10^{-3}$		$\times 10^{-3}$		$\times 10^{-3}$		$\times 10^{-3}$
$^{207}\text{Pb}/^{206}\text{Pb}$	0.9250	a = 143.9 (142.4, 145.5)	0.9517	a = 188.3 (186.8, 189.9)	0.9136	a = 103.9 (102.8, 105.0)	0.4027	a = 66.65 (61.49, 71.81)
		b = 16.23 (16.02, 16.43)		b = 22.69 (22.48, 22.90)		b = 12.07 (11.92, 12.22)		b = 7.705 (7.043, 8.368)
		c = 6.459 (3.653, 9.266)		c = 0.5763 (-0.9437, 2.096)		c = -11.25 (-13.08, -9.422)		c = 86.60 (38.92, 134.3)
$^{208}\text{Pb}/^{232}\text{Th}$	0.9279	a = 58.61 (56.99, 60.22)	0.7579	a = 117.8 (106.2, 129.3)	0.6576	a = 111.9 (92.07, 131.7)	0.1662	a = 20.68 (17.60, 23.76)
		b = 3.751 (3.591, 3.911)		b = 2.585 (2.245, 2.925)		b = 4.332 (3.303, 5.362)		b = 10.43 (6.889, 13.97)
		$\times 10^{-4}$		$\times 10^{-4}$		$\times 10^{-4}$		$\times 10^{-4}$

85 **Note: Regression equations are the same as those in Table 3.****Table S3. Intersection of age error curves (unit: Ma)**

Intersection of age error curves	All methods	LA-ICP-MS	SHRIMP	SIMS	TIMS
$^{206}\text{Pb}/^{238}\text{U}$ and $^{207}\text{Pb}/^{235}\text{U}$	1162.54	1177.34	1197.74	748.07	971.38
$^{206}\text{Pb}/^{238}\text{U}$ and $^{207}\text{Pb}/^{206}\text{Pb}$	1795.50	1933.79	1619.01	1273.76	1182.52
$^{207}\text{Pb}/^{235}\text{U}$ and $^{207}\text{Pb}/^{206}\text{Pb}$	2390.44	2694.25	1956.91	1548.17	1295.16

4. References.

- 90 Arndt, N. and Davaille, A.: Episodic Earth evolution, *Tectonophysics*, 609, 661-674, 10.1016/j.tecto.2013.07.002, 2013.
- Keller, C. B. and Schoene, B.: Statistical geochemistry reveals disruption in secular lithospheric evolution about 2.5 Gyr ago, *Nature*, 485, 490-493, 10.1038/nature11024, 2012.
- Mehra, A., Keller, C., Zhang, T., Tosca, N., McLennan, S., Sperling, E., Farrell, U., Brocks, J., Canfield, D., and Cole, D.:
95 Curation and analysis of global sedimentary geochemical data to inform earth history, *GSA Today*, 31, 4-10,
10.1130/GSATG484A.1, 2021.
- Puetz, S. J. and Spencer, C. J.: Evaluating U-Pb accuracy and precision by comparing zircon ages from 12 standards using
TIMS and LA-ICP-MS methods, *Geosystems and Geoenvironment*, 2, 100177, 10.1016/j.geogeo.2022.100177, 2023.
- Puetz, S. J., Spencer, C. J., and Ganade, C. E.: Analyses from a validated global U-Pb detrital zircon database: Enhanced
100 methods for filtering discordant U-Pb zircon analyses and optimizing crystallization age estimates, *Earth-Science
Reviews*, 220, 103745, 10.1016/j.earscirev.2021.103745, 2021.
- Wu, Y., Fang, X., Jiang, L., Song, B., Han, B., Li, M., and Ji, J.: Very long-term periodicity of episodic zircon production
and Earth system evolution, *Earth-Science Reviews*, 104164, 10.1016/j.earscirev.2022.104164, 2022.